COMMENTS ON THE BEHAVIOR OF α_1 IN MAIN INJECTOR γ_t JUMP SCHEMES

S.A. Bogacz and S. Peggs

Accelerator Physics Department,
Fermi National Accelerator Laboratory*
P.O. Box 500, Batavia, IL 60510

October 1990

Tracking studies of transition crossing in the Main Injector have shown that the Johnsen effect is the dominant cause of beam loss end emittance blow up. To suppress this effect one has to have control over α_1 (dispersion of the momentum compaction factor α). Various γ_t jump configurations are examined and the resulting changes in α_1 are assessed. These results are further validated by comparison between the simulation and simple analytic α_1-formulas derived for a model FODO lattice. The lattice assumes full chromaticity compensation and presence of eddy current sextupole component. The last scheme seems to be very promising as one can regard the strength of eddy current sextupole family as an external "knob" to control values of α_1.

---

*Operated by the Universities Research Association, Inc., under a contract with the U.S. Department of Energy

INTRODUCTION

Tracking studies of transition crossing in the Main Injector and other Fermilab accelerators, using the code ESME, have shown that the Johnsen effect is the dominant cause of beam loss and emittance blow up [1,2]. This effect is rooted in the variation of γ_t the transition gamma, with $\delta = \frac{\Delta p}{p_0}$, the off-momentum parameter. Although transition crossing may be well tuned for the nominal particle, perhaps with an "instantaneous" snap of the radio frequency phase and a γ_t jump scheme, it is not trivial to satisfy the needs of a momentum spectrum of particles. In general, individual off-momentum particles cross transition either too early, or too late. This leads to particle loss and longitudinal emittance growth which is independent of the intensity of the bunch under consideration. A useful parameter characterizing the strength of this effect is the Johnsen time, T_J, which represents the root mean square spread of the transition crossing time [3-6]. This time is proportional to $\frac{\sigma_p}{p}$, the root mean square momentum spread.

The Johnsen time is directly related to the lattice parameter α_1, which is defined by the equation

$$\frac{\Delta C}{C_0} = \alpha_0 \, \delta + \alpha_1 \, \delta^2 + ... \qquad (1)$$

where C_0 is the nominal closed orbit path length, and ΔC is the increase in path length for an off momentum particle. Unfortunately, more than one definition of α_1 is common in the literature, as discussed in the Appendix. Let the reader beware! As defined here, the coefficients α_0 and α_1 are geometrical properties of the lattice, given by

$$\alpha_0 = \frac{2\pi}{C_0} < \eta_0 > , \quad \alpha_1 = \frac{2\pi}{C_0} < \eta_1 > \qquad (2)$$

where angle brackets <...> denote averaging weighted by bend angle. The quantities being averaged are component dispersions in a momentum expansion of the total dispersion. That is,

$$\eta(s) = \eta_0(s) + \eta_1(s)\,\delta + ... \tag{3}$$

explicitly showing the dependence of the dispersion on s, the accelerator azimuth.

Transition comes for a particle with a macroscopic momentum displacement Δp when a neighboring trajectory, infinitesimally displaced by dp, has the same revolution frequency. If it is assumed that equation 1 is exact (α_2, et cetera, are zero), then it can be shown that the exact condition for transition crossing becomes

$$\frac{1}{\gamma_t^2} = \frac{\alpha_0 + 2\,\alpha_1\,\delta}{1 + \alpha_0\,\delta + \alpha_1\,\delta^2}(1 + \delta) \tag{4}$$

Keeping only first order terms in δ, this equation can be rearranged to give the γ of the off-momentum particle as it passes through transition,

$$\gamma_t = \gamma_{t0}\left[\,1 - \left(\frac{1}{2} + \frac{\alpha_1}{\alpha_0} - \frac{\alpha_0}{2}\right)\delta\,\right] \tag{5}$$

Here γ_{t0} is the γ of the nominal particle as it passes through its transition. However, a more useful quantity is the γ of the nominal particle at the time that the off momentum particle passes through transition. This is given by

$$\gamma_0(\delta) = \gamma_{t0}\left[\,1 - \delta\,\right] \tag{6}$$

so that the Johnsen time becomes

$$T_J = \frac{\gamma_0\left(\frac{\sigma_p}{p}\right)}{\dot{\gamma}} = \frac{\gamma_{t0}}{\dot{\gamma}}\left[\,\frac{3}{2} + \frac{\alpha_1}{\alpha_0} - \frac{\alpha_0}{2}\,\right]\frac{\sigma_p}{p} \tag{7}$$

where $\dot{\gamma}$ is the ramp rate through transition. The Main Injector, for example, has (approximately) $\gamma_{t0} = 20$, $\dot{\gamma} = 240\ \text{sec}^{-1}$, $\alpha_1 = 0$, and $\frac{\sigma_p}{p} = 5.10^{-3}$, so that T_J is about 0.6 milliseconds, or about 60 accelerator turns.

Clearly, if it is not possible to control the Johnsen time, it is futile to arrange for a γ_t jump on a time scale much faster than this. Also, analysis of how α_1 changes should be included as an additional topic in the evaluation of γ_t jump schemes, to ensure that T_J does not rise significantly. On the positive side, if it is possible to measure and control α_1, then it should be possible to make $T_J = 0$, and ameliorate the damage done by the Johnsen effect, by setting

$$\alpha_1 = -\frac{3}{2}\alpha_0 + \frac{1}{2}\alpha_0{}^2 \tag{8}$$

The second term on the right is essentially negligible. The improvement in transition performance might then be dramatic enough that a γ_t jump would no longer be necessary. This may be true especially if α_1 control is combined with rf gymnastic tricks, such as the use of a synchronous phase of 90^0 and a second harmonic cavity, as now being discussed elsewhere [7].

THE DIFFERENTIAL EQUATION FOR THE SUM DISPERSION, η_+

The horizontal closed orbit h(s) is found by solving the differential equation

$$h'' + \frac{K(s)}{1+\delta} h + \frac{S(s)}{1+\delta} h^2 = G(1 - \frac{1}{1+\delta}) \tag{9}$$

with periodic boundary conditions. A prime indicates differentiation with respect to s, K is the quadrupole strength, S is the sextupole strength, and G is the dipole bending strength. If h is expanded in a dispersion function series

$$h = x_{CO} + \eta_0 + \eta_1 \delta + ... \tag{10}$$

which is substituted into 9, three differential equations are obtained by grouping terms according to their order in δ, up to second order. The solution of the lowest order equation is trivial when there are no closed orbit perturbations, $x_{CO} = 0$, so that the remaining two equations become

$$\eta_0'' + K \eta_0 = G \tag{11a}$$

$$\eta_1'' + K \eta_1 = - G + K \eta_0 - S \eta_0^2 \tag{11b}$$

The differential equation for the convenient "sum dispersion", defined by

$$\eta_+ = \eta_0 + \eta_1 \tag{12}$$

is obtained by adding equations 11a and 11b, to give

$$\eta_+'' + K \eta_+ = K \eta_0 - S \eta_0^2 \tag{13}$$

The source terms on the right hand side of equation 13 depend only on the solution of 11a for the "normal" dispersion. Solving this differential equation is slightly easier than solving 11b for η_1, and a subsequent calculation of $<\eta_+>$ allows for a direct knowledge of α_1, since

$$\alpha_1 = \alpha_+ - \alpha_0 = \frac{2\pi}{C_0} < \eta_+ > - \alpha_0 \tag{14}$$

In order to set the Johnsen time to zero, therefore, it is necessary to set

$$\alpha_+ = -\frac{1}{2}\alpha_0 \tag{15}$$

The next section solves equation 13 in a naive FODO representation of the Main Injector, and quantitatively identifies the major factors which affect η_+ and hence α_+ and α_1 .

SOLUTION IN A FODO LATTICE WITH EDDY CURRENT SEXTUPOLES

Suppose that an accelerator like the Main Injector is represented as made up purely of FODO cells, as illustrated in Figure 1. The quadrupoles are thin, and there is no drift space. All of the half cell length L is filled with two identical dipoles of bend radius R, which are separated by a thin sextupole representing the field due to vacuum chamber eddy currents, induced during the ramp. There are also two thin chromatic correction sextupoles per half cell, immediately adjacent to the focussing and defocusing quadrupoles. The strength of the (half) quadrupoles is $\pm q$, and of the sextupoles is g_F, g_D, and g_E, where

$$q = \frac{s}{L} = \frac{\sin(\phi_{1/2})}{L} \tag{16a}$$

$$g_F = \frac{(S_F \Delta l)\, \eta_{0F}}{q}, \quad g_E = \frac{(S_E \Delta l)\, \eta_{0E}}{q}, \quad g_D = \frac{(S_D \Delta l)\, \eta_{0D}}{q} \tag{16b}$$

In these expressions $\phi_{1/2}$ is the half cell phase advance (about 44 degrees in the Main Injector), while S_F and η_{0F} (for example) are the sextupole gradient and the lowest order dispersion, at the F chromatic sextupole of thin length Δl. From here on s, as defined in equation 16a, is the sine of the half cell phase advance, and not the azimuthal coordinate.

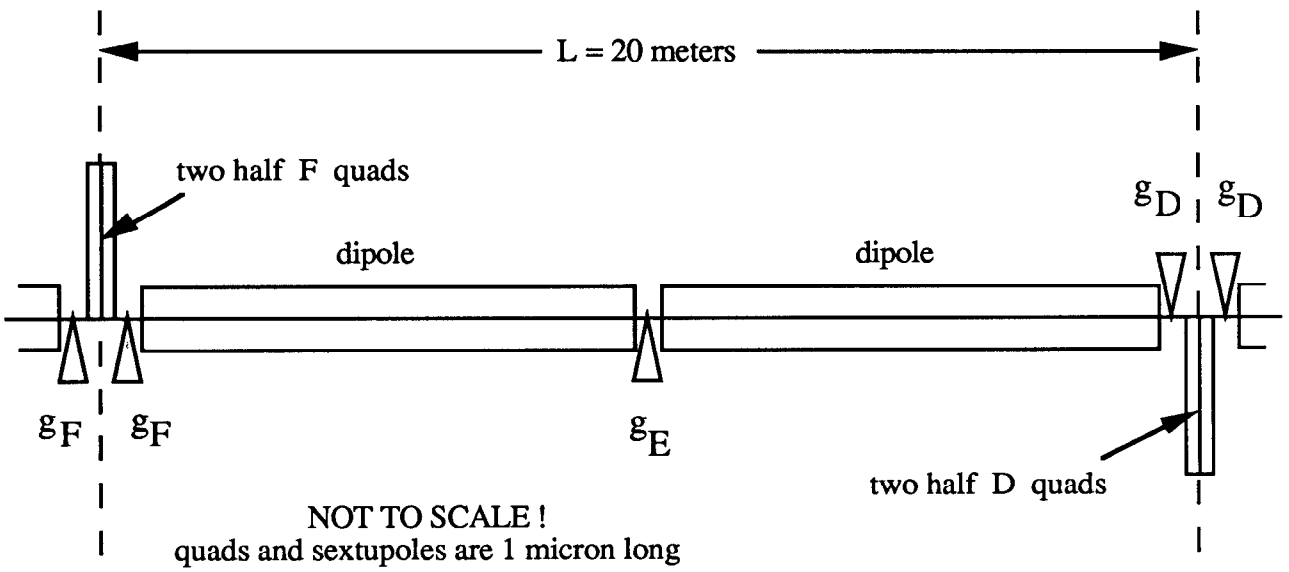

Figure 1 Half of a FODO cell, in a model representing the Main Injector with three sextupole families.

Using these convenient definitions, it can be shown by solving equation 13 that the matched values of the sum dispersion at F, E, and D are

$$\eta_{+F} = \frac{1}{s}\left[\eta_{0F}(1+s)(1-g_F) - \eta_{0D}(1+g_D) - \frac{\eta_{0E}}{2}(2+s)g_E\right] \tag{17a}$$

$$\eta_{+E} = \frac{1}{2s}\left[\eta_{0F}(2+s)(1-g_F) - \eta_{0D}(2-s)(1+g_D) - \frac{\eta_{0E}}{2}(2+s)(2-s)g_E\right] \tag{17b}$$

$$\eta_{+D} = \frac{1}{s}\left[\eta_{0F}(1-g_F) - \eta_{0D}(1-s)(1+g_D) - \frac{\eta_{0E}}{2}(2-s)g_E\right] \tag{17c}$$

Note that $\eta_{+E} = \frac{1}{2}(\eta_{+F} + \eta_{+D})$ when $g_E = 0$, as required by equation 13, which says that the sum dispersion propagates linearly in a quadrupole and sextupole free region. These solutions can be combined to evaluate α_+, since

$$\alpha_+ = \frac{\langle\eta_+\rangle}{R} = \frac{1}{4R}(\eta_{+F} + 2\eta_{+E} + \eta_{+D}) \tag{18}$$

$$= \frac{1}{2sR}\left[\eta_{0F}(2+s)(1-g_F) - \eta_{0D}(2-s)(1+g_D) - \frac{\eta_{0E}}{4}(8-s^2)g_E\right]$$

This expression becomes more direct when the η_0 terms are replaced by their explicit matched solutions

$$\eta_{0F} = \frac{L^2}{R}\frac{2+s}{2s^2} \tag{19a}$$

$$\eta_{0E} = \frac{L^2}{R}\frac{8-s^2}{8s^2} \tag{19b}$$

$$\eta_{0D} = \frac{L^2}{R}\frac{2-s}{2s^2} \tag{19c}$$

Thus, an alternative form for equation 18, parameterized primarily by the sextupoles strengths, is

$$\alpha_+ = \frac{L^2}{R^2}\frac{1}{4s^3}\left[\, 8s - (2+s)^2\, g_F - (2-s)^2\, g_D - \frac{(8-s^2)^2}{16}\, g_E \,\right] \tag{20}$$

In order to take stock of the meaning of equation 20, consider the case when only the F and D sextupoles are turned on, at a strength to correct for f times the natural chromaticity.

Independent of the strength of any sextupoles, it can easily be shown that

$$\alpha_0 = \frac{L^2}{R^2}\frac{1}{s^2}\left[\, 1 - \frac{s^2}{12} \,\right] \tag{21}$$

It can also easily be shown that, in order to correct f times the natural FODO chromaticity, $g_F = \frac{f}{2}$ and $g_D = -\frac{f}{2}$, demonstrating the utility of the natural scaling that was introduced, apparently arbitrarily, in equation 16b. Substituting these values (and $g_E = 0$) into equation 20 gives

$$\alpha_+ = \frac{L^2}{R^2}\frac{1}{s^2}\left[\, 2 - f \,\right] \tag{22}$$

which immediately leads to

$$\alpha_1 = \frac{L^2}{R^2}\frac{1}{s^2}\left[\, 1 - f + \frac{s^2}{12} \,\right] \tag{23}$$

showing that $\alpha_1 << \alpha_0$ in a simple FODO lattice with the net chromaticity set to zero (f = 1).

CONTROLLING α_1 WITH SEXTUPOLES

The middle sextupole, of strength g_E, can be thought of in (at least) two ways. In the first point of view, it represents the sextupole field caused by eddy currents induced in the vacuum chamber of the dipoles. (Note in passing that this representation is not perfect, since the changes in horizontal and vertical chromaticities are modeled as equal and opposite, whereas in reality they are unequal.) In the second point of view, g_E represents a free knob with which η_+, and hence also α_+ and α_1, can be controlled. The reader may choose either perspective in what follows - or a combination, in which g_E represents the net strength after an independent correction sextupole is powered to over or under compensate the local eddy current sextupole fields. From any perspective, the task of setting the net chromaticities to their desired values is left to the F and D sextupoles. For the sake of a semi-quantitative interpretation, suppose that the F and D sextupoles have their strengths set to compensate for the sum of the chromaticity induced by an eddy current sextupole of strength g_E, plus f times the natural chromaticity.

In this case it is readily shown that the F and D sextupole strengths are given by

$$g_F = \frac{f}{2} - \frac{2 - s^2}{4} g_E \tag{24a}$$

$$g_D = -\frac{f}{2} - \frac{2 - s^2}{4} g_E \tag{24b}$$

Substituting these expressions into equation 20 gives

$$\alpha_+ = \frac{L^2}{R^2}\frac{1}{s^2}\left[(2 - f) - \left(\frac{3}{8}\right)^2 s^3 g_E \right] \tag{25}$$

or, equivalently,

$$\alpha_1 = \frac{L^2}{R^2}\frac{1}{s^2}\left[(1 - f + \frac{s^2}{12}) - \left(\frac{3}{8}\right)^2 s^3 g_E \right] \tag{26}$$

These equations reduce to equations 22 and 23 when $g_E = 0$, as they should. If it is also assumed that the phase advance per cell is (approximately) 90^0, then $s = 1/\sqrt{2}$, and the three compaction factors become simply

$$\alpha_0 = \frac{L^2}{R^2} \times 1.917 \tag{27a}$$

$$\alpha_+ = \frac{L^2}{R^2}\left[4 - 2f - 0.0994 \times g_E \right] \tag{27b}$$

$$\alpha_1 = \frac{L^2}{R^2}\left[2.083 - 2f - 0.0994 \times g_E \right] \tag{27c}$$

Typical values for g_E due to eddy current sextupoles in the Main Injector are 2 or 3, showing through equation 24 that they more or less dominate the strength of the F and D families [8].

To test the results of equation 27, and to gain some insight into the prospect of controlling α_1 in the Main Injector, consider a lattice made up of 80 simple FODO cells. In the parameterization introduced above the half cell has a length L = 20 meters, and is filled with dipoles of bending radius $R = 3200/2\pi = 509.30$ meters. Figure 2 summarizes results of simulations of such a lattice, using the program MAD (version 8.17)[9] to study the variation in closed orbit path-length as a function of $\Delta p/p$, over a range from -0.003 to $+0.003$. The momentum compaction factor α_P defined by equation A-3 in the Appendix is plotted. Equations A-3 and A-6 are then used to yield values of α_0 and α_1, ready for comparison with the analytic predictions of equations 27a and 27c. Eddy current multipoles higher than sextupole are neglected.

Three cases are considered; no eddy currents with and without complete compensation of the natural chromaticities, $(f,g_E) = (0,0)$ and $(1,0)$, and then complete chromaticity compensation with large but realistic eddy current sextupole strengths, $(f,g_E) = (1,5)$. Each of the plots is linear to a very good approximation, showing that α_0 and α_1 are the dominant coefficients in the α_P expansion. Table 1 shows excellent agreement between the simulated and the predicted values of α_0 and α_1, except for what appears to be a systematic error in α_1 of $0.120 \pm 0.005 \times 10^{-3}$. The source of this small difference is not known, but is not considered to be important. Further comparisons using other design programs are anticipated, to see if the error persists.

If the sextupole family strength parameter g_E is regarded as an external "knob" to control values of α_1, the inevitable conclusion is that the sensitivity to the family is too weak to reduce the Johnsen time to zero, short of using a very large strength or relinquishing control of the net chromaticities. Recall from equation 8 and from Table 1 that the desired value of α_1 is approximately -4.5, but notice that the α_1 sensitivity coefficient in equation 27c is only 0.0994, disappointingly small. This is reflected in the minor changes of α_1 between the second and third rows of Table 1.

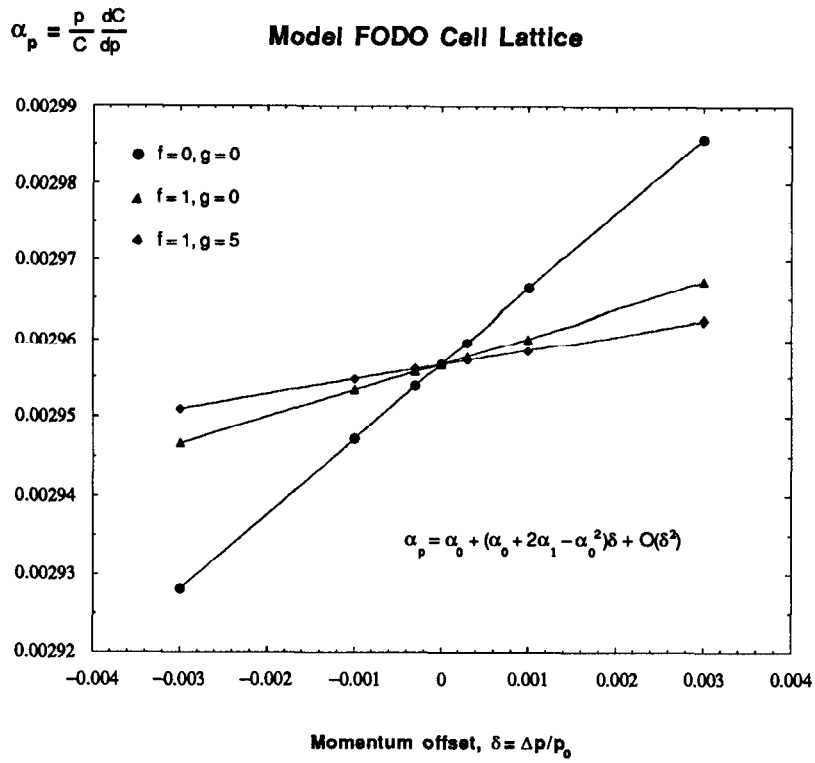

Figure 2 Numerical simulation of momentum compaction factor variation with δ for three configurations of eddy current and chromaticity compensation sextupole strengths.

(f,g_E)	α_0		α_1	
	predicted ($\times 10^{-3}$)	simulated ($\times 10^{-3}$)	predicted ($\times 10^{-3}$)	simulated ($\times 10^{-3}$)
(0,0)	2.956	2.956	3.213	3.332
(1,0)	2.956	2.956	.129	.244
(1,5)	2.956	2.956	−.638	−.512

Table 1 Comparison of predicted and simulated α_0 and α_1 values.

Investigations are currently under way to find an optical configuration that will significantly increase the orthogonality of the three families beyond the unfortunate results of the FODO lattice. An apparently promising candidate involves the introduction of a dispersion wave in the arcs of the Main Injector, around transition time. This begins to resemble an unmatched γ_t jump scheme - except that the lattice perturbation can be introduced slowly, and that the needed size of the dispersion wave is expected to be relatively modest.

BEHAVIOR OF MATCHED AND UNMATCHED γ_t JUMP SCHEMES

The satisfactory agreement between MAD817 simulations and analytic predictions reported in the previous section, for the simple case of a FODO lattice, encourages the use of the program to study the behavior of momentum compaction factors for more realistic Main Injector lattices, where analytic results are no longer tractable. Here we consider two families of Main Injector lattices representing matched and unmatched γ_t jump schemes. These schemes are described in detail elsewhere [10]. It is important to check that the resulting change of α_1 does not greatly affect the Johnsen time T_J, extending the variation of transition crossing time for different parts of a bunch.

The simulation places one thin eddy current sextupoles of strength g_E at the middle of each dipole, with a multipole strength of $b_2 = 0.561\ m^{-2}$. Two families of chromatic sextupoles are used to compensate for both natural and eddy current chromaticities. It is assumed, for the sake of definiteness, that the F and D sextupole strengths are not changed while jumping through transition. Figure 3a summarizes the behavior of the matched scheme with bipolar ($\Delta\gamma_t = \pm\ 0.65$) and unipolar ($\Delta\gamma_t = -1.3$) excitations. Figure 3b examines an unmatched unipolar excitation - a bipolar jump is not possible in this scheme. The linear character of $\alpha_P(\delta)$ in the realistic range $\delta = -0.01$ to $+0.01$ is apparent in all cases. Note that the vertical scales are significantly different in the two figures - compare the same $\Delta\gamma_t = 0$ case shown in both figures.

Table 2 summarizes the simulation results. Since the arcs in a matched scheme are essentially just a sequence of FODO cells slightly retuned by a quadrupole perturbation, it is expected to produce qualitatively the same results as the FODO lattice in the previous section. Indeed, the values of α_1 recorded in Table 2 are an order of magnitude smaller than α_0, and do not pose any danger to the Johnsen time. By contrast, the unmatched scheme produces large value of $\alpha_1 \approx 1.68\ \alpha_0$, which, according to equation 8, more than doubles the Johnsen time. Also included in Table 2 are the uncorrected chromaticities, ξ_H and ξ_V, with the F and D sextupoles turned off, but with the eddy current sextupoles turned on.

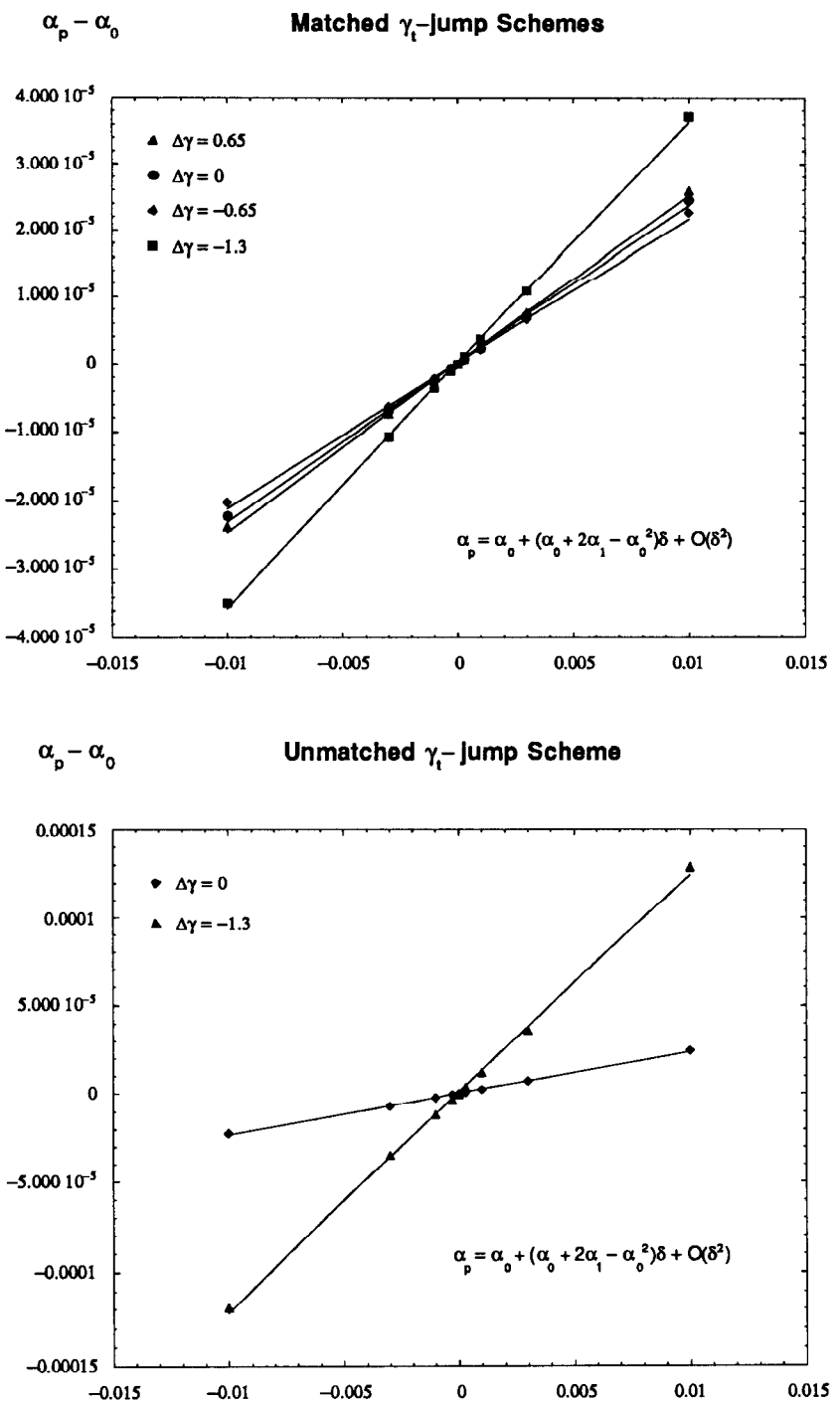

Figure 3 Numerical simulation of momentum compaction factor variation versus δ carried out for various γ_t–jump configurations. The simulation includes eddy current sextupoles and full chromaticity compensation.

Scheme	$\Delta\gamma_t$	α_0 ($\times 10^{-3}$)	α_1 ($\times 10^{-3}$)	ξ_H uncorrected	ξ_V uncorrected
Matched	.65	2.23	.14	−10.6	−46.4
	.0	2.37	−.01	−7.6	−47.3
	−.65	2.53	−.19	−6.4	−48.3
	−1.3	2.70	−.45	−8.5	−49.7
Unmatched	.0	2.37	−.01	−7.6	−47.3
	−1.3	2.70	−4.82	−3.9	−50.1

Table 2 The behavior of momentum compaction coefficients, and of the uncorrected chromaticities, in matched and unmatched Main Injector transition jump schemes.

CONCLUSIONS

General analytical expressions are reported above for the variation of the dispersion function to first order in the off-momentum parameter δ, and for the variation of the closed orbit circumference to second order. This makes it possible to evaluate how the critical Johnsen time (for example) depends on effects like eddy current sextupoles in the Main Injector dipoles, or on transition jump configurations. In the simple but relevant case of a FODO lattice representation of the Main Injector, analytic results are in good quantitative agreement with a lattice design code.

If there is no γ_t jump in the Main Injector, the Johnsen time is typically expected to be about 0.6 milliseconds, or about 60 machine turns. There is no benefit from turning on a γ_t jump much faster than this. Examination of nominal Main Injector transition jump schemes reveals that a matched scheme produces little change in the Johnsen time, but that T_J is more than doubled in the unmatched scheme.

A third family of sextupoles might be used to deliberately and practically control the Johnsen time, without modifying the nominal transition momentum. (Two other sextupole families are used to achieve the desired net chromaticities.) Such control, especially when used in conjunction with rf gymnastics, may make transition crossing so innocuous that it becomes unnecessary to include a transition jump in Main Injector designs.

However, the Johnsen time in a FODO lattice is quite insensitive to a third family of sextupoles located at the middle of the half cells. The good news is, then, that eddy current sextupoles are not expected to significantly affect transition crossing performance. The bad news is that using mid-cell sextupoles to control the Johnsen time is not practical. Continuing investigations suggest that a modest dispersion wave significantly improves the orthogonality of three families of sextupoles.

REFERENCES

1) S.A. Bogacz, *Transition crossing in the Main Injector - ESME simulation*, Proceedings of the F III Instability Workshop, Fermilab, July 1990.

2) I. Kourbanis and K.Y. Ng, *Main Ring transition crossing simulations*, Proceedings of the F III Instability Workshop, Fermilab, July 1990.

3) K. Johnsen, *Effects of non-linearities on the phase transition*, CERN symposium on high energy accelerators and pion physics, Vol. 1, p. 106, 1956.

4) A. Sorenssen, *Crossing the phase transition in strong focusing proton synchrotrons*, Particle Accelerators Vol. 6, pp. 141-165, 1975. This is an excellent review article.

5) P. Faugeras, A. Faugier, J. Gareyte, *Effets chromatiques et passage de la transition a grand $\Delta p/p$*, CERN SPS Improvement note No. 130, 1978.

6) S. Peggs, *Transition crossing time shifts*, Fermilab note AP 90-004, 1990.

7) J. MacLachlan and J. Griffin, private communication.

8) J-F Ostiguy, *Eddy current induced multipoles in the Main Injector*, Fermilab note MI-0037, October 1990.

9) H. Grote and C. Iselin, *The MAD program users reference guide*, CERN note CERN/SL/90-13 (AP), 1990.

10) S.A. Bogacz, F. Harfoush, and S. Peggs, *A comparison of matched and unmatched γ_t jump schemes in the Main Injector*, Proceedings of the F III Instability Workshop, Fermilab, July 1990.

APPENDIX – RELATIONS BETWEEN α_1 AND OTHER PARAMETERS

For reference purposes, this appendix describes how the three definitions of α_1 and the one definition of α_p, all of which are common in the literature, are related. It has already been released as Fermilab Main Injector note MI-0038, by MacLachlan, Ng, and Peggs, with only minor differences.

The "circumference" definition of α_1, as defined in equation 1 and used throughout above, comes from expanding the difference in the circumference of the closed orbit, $\Delta C = C - C_0$, as a polynomial in the off momentum parameter, $\delta = (p - p_0) / p_0$,

$$\frac{\Delta C}{C_0} = \alpha_0 \, \delta + \alpha_{C1} \, \delta^2 + ... \qquad \text{(A-1)}$$

The definition introduced by Johnsen is very similar

$$\frac{\Delta C}{C_0} = \alpha_0 \, \delta + \alpha_0 \, \alpha_{J1} \, \delta^2 + ... \qquad \text{(A-2)}$$

The variation of the transition energy γ_t with δ is directly described by α_p, defined through

$$\alpha_p(\delta) = \frac{1}{\gamma_t^2(\delta)} = \frac{p}{C} \frac{dC}{dp} = \alpha_0 + \alpha_{E1} \, \delta + ... \qquad \text{(A-3)}$$

This introduces the ESME definition of α_1.

Note that equation A-3 represents the <u>local</u> derivative at some momentum p. WARNING - when used with a constant momentum offset, some lattice design codes return $\alpha_p(\delta)$, but some return

$$\frac{p_0}{C_0} \frac{dC}{dp} = \alpha_0 + \alpha_{C1} \, \delta + ... \qquad \text{(A-4)}$$

Comparing equations A-1 and A-2 gives

$$\alpha_{F1} = \frac{\alpha_{C1}}{\alpha_0} \tag{A-5}$$

Performing the differentiation in equation A-3 and expanding gives

$$\alpha_{E1} = \alpha_0 + 2\,\alpha_{C1} - \alpha_0^2 \tag{A-6}$$

Although this paper has conveniently taken equation 1 to define $\alpha_1 = \alpha_{C1}$, the selection is (somewhat) arbitrary. The reader is NOT implored to adopt one or another of the definitions introduced here, but rather is asked to be careful to specify which definition he or she is using. He or she IS implored not to invent any more definitions for α_1 .